

Research Article

Hyperbaric oxygen-assisted melatonin therapy protects the heart from acute ischemia-reperfusion injury

Han-Tan Chai ^{^1}, Jui-Ning Yeh ^{^2,3}, Pei-Hsun Sung ^{1,4,5}, John Y Chiang ^{6,7}, Fan-Yen Lee ⁸, Hon-Kan Yip ^{*1,4,5,9,10,11}

¹Division of Cardiology, Department of Internal Medicine, Kaohsiung Chang Gung Memorial Hospital and Chang Gung University College of Medicine, Kaohsiung, 83301, Taiwan.

²Institute of Nephrology and Blood Purification, the First Affiliated Hospital of Jinan University, Jinan University, Guangzhou 510632, China

³Department of Cardiology, The First Affiliated Hospital, Jinan University, Guangzhou, 510632, China.

⁴Institute for Translational Research in Biomedicine; ⁵Center for Shockwave Medicine and Tissue Engineering, Kaohsiung Chang Gung Memorial Hospital, Kaohsiung 83301, Taiwan

⁶Department of Computer Science and Engineering, National Sun Yat-Sen University, Kaohsiung 804201, Taiwan.

⁷Department of Healthcare Administration and Medical Informatics, Kaohsiung Medical University, Kaohsiung 80708, Taiwan.

⁸Division of Thoracic and Cardiovascular Surgery, Department of Surgery, Kaohsiung Chang Gung Memorial Hospital and Chang Gung University College of Medicine Kaohsiung 83301, Taiwan

⁹Department of Medical Research, China Medical University Hospital, China Medical University, Taichung 40402, Taiwan

¹⁰Department of Nursing, Asia University, Taichung 41354, Taiwan

¹¹Division of Cardiology, Department of Internal Medicine, Xiamen Chang Gung Hospital, Xiamen 361028, Fujian, China

[^]Equal contribution

^{*}Correspondence: han.gung@msa.hinet.net, Tel: 886-7-7317123 ext. 8301

Running title: HBO and melatonin against IR

Received: February 11, 2022; Accepted: June 3, 2022

ABSTRACT

In this study we have examined whether hyperbaric oxygen (HBO)-assisted melatonin (Mel) therapy effectively preserves the heart function against ischemia (40-min)-reperfusion (IR) injury. First, the *in vitro* study has been performed by use of cell culture. H9C2 cells were treated as groups: A (H9C2) (without any treatment), B (H9C2+IR), C (H9C2+IR+HBO), D [H9C2+IR+Melatonin (50 μ M)] and E (H9C2+IR+Melatonin+HBO). The result showed that the protein expressions of oxidative-stress (NOX-1/NOX-2)/inflammatory (TNF- α /NF- κ B)/apoptotic (mitochondrial-Bax/cleaved-caspase-3/cleaved-PARP) and cellular levels of DNA/mitochondrial-damaged (γ -H2AX/XRCC1-CD90+/cytosolic-cytochrome-C) biomarker were significantly increased in group B compared to control group A. These biomarkers were significantly reduced in group C, D and E compared to groups B with the significantly higher reduction in group E than that in groups C and D ($p < 0.001$). In the *in vivo* study, adult-male SD rats ($n=40$) were equally divided into group 1 (sham-operated-control), group 2 (IR), group

3 (IR+HBO therapy at 1.5/24/48h after IR procedure), group 4 [IR+Mel (50mg/kg at 1.5h, followed by 20mg/kg and at days 1/2/3 after IR)] and group 5 (IR+HBO-Mel) and the heart was harvested at 72h after IR. The result showed that at 72h, the circulating levels of endothelial-progenitor-cells (c-kit-CD31+/CD31-sca-1+/KDR-CD34+/VE-Cadherin-CD34+) were lowest in group 2, highest in group 5 and followed by groups 3 > 4 > 1. The significant differences were present between each two matched groups ($p < 0.0001$). The protein expressions of angiogenic factors (SDF-1 α /CXCR4/VEGF/HIF- α) were progressively increased from groups 1 to 5 with significant differences. The protein expressions of apoptosis (mitochondrial-Bax/cleaved-caspase-3/cleaved-PARP)/fibrosis (TGF- β /Smad3)/oxidative-stress (NOX-1/NOX-2/oxidized protein)/inflammation (TNF- α /IL-1 β /MMP-9) and infarct/fibrotic areas were significantly increased in group 2 compared to the control group 1. All these parameters were significantly reduced in groups 3-5 compared to group 2 with significantly lowest level in group 5 among groups 3-5 ($p < 0.01$), whereas the left-ventricular-ejection-fraction exhibited an opposite pattern compared to the inflammatory factors. In conclusion, HBO-Mel therapy offered a synergic benefit for protecting the heart from IR injury.

Key words: ischemia-reperfusion, melatonin, hyperbaric oxygen, inflammation, oxidative stress, mitochondrial damage, apoptosis

1. INTRODUCTION

Despite state-of-the-art advances in pharmacotherapy, instrument refinement for intervention, maturation of skillful techniques, continuous guideline renewals for education as well as innovation and fruition for new mechanical devices, the cardiovascular diseases (CVDs) remain the leading cause of death worldwide (1-5). In fact, CVDs are constituted by a variety of different disease entities, such as obstructive coronary artery disease, valvular heart disease, dilated cardiomyopathy, hypertrophic cardiomyopathy, viral infection (i.e., acute myocarditis) and myocardial injury by ischemia-reperfusion (IR). Of these etiologies, acute myocardial IR injury is one of the principal contributors for myocardial damage, loss of myocardium, resulting in left ventricular (LV) dysfunction and heart failure (HF).

Undoubtedly, myocardial IR injury is frequently encountered due to cardiac surgery, organ transplantation, cardiogenic shock, prolonged resuscitation or circulatory arrest of different etiologies as well as no-reflow phenomenon during percutaneous coronary intervention (6-10). On the other hand, although reperfusion of the ischemic myocardium plays the key role to minimize myocardial damage, yet reperfusion is also well-recognized for its deleterious side-effects (7) due to the generations of reactive oxygen species (ROS) which causes oxidative stress, and vigorous inflammatory and immune reactions (7, 11-18). Of particular importance is that the ROS generated, interacting with mitochondria, not only will damage the mitochondria but can further accelerate ROS/free radical generation and ultimately form a vicious cycle to cause cell apoptosis and death. Regrettably, there is currently still no effective treatment on IR-induced myocardial damage. Accordingly, to find out a new modality with safety and efficacy is utmost important to cardiologists and patients.

Melatonin (Mel), an indoleamine mainly secreted from the pineal gland with a potent and durable free radical scavenging capacity, has been demonstrated to play a fundamental role in maintaining cell membrane stability and ensuring cell survival in toxic environment mainly through a reduction of organ susceptibility to oxidative stress and inflammation (19-23). Our previous and recent studies have further identified that Mel treatment markedly protected the major organs of liver, lung and small bowel against acute IR injury (19, 22-25). Additionally,

hyperbaric oxygen (HBO) therapy is a traditional therapy for patients with ischemic peripheral arterial occluded disease (PAOD) (26). The HBO therapy involves in the improvement of ischemic PAOD and restoration of its blood flow. Thus, its underlying mechanism has been proposed to mainly increase vascular wall permeability and productions of hypoxic inducible factor (HIF)-1 α and stromal cell-derived factor (SDF)-1 α in both ischemic region and systemic circulation, resulting in enhancement of angiogenesis/neovascularization in the ischemic area (27-29). Based on the aforementioned evidence (19-29), it was reasonable to believe that a combined therapy of HBO and Mel would be superior to either one alone for improving the heart function after acute myocardial IR injury. To test this hypothesis, the *in vitro* (cell culture) and *in vivo* (rats) studies have been performed in the current study.

2. MATERIALS AND METHODS

2.1 Ethics.

All animal procedures were approved by the Institute of Animal Care and Use Committee at Kaohsiung Chang Gung Memorial Hospital (Affidavit of Approval of Animal Use Protocol No. 2018061402) and performed in accordance with the Guide for the Care and Use of Laboratory Animals.

Animals were housed in an Association for Assessment and Accreditation of Laboratory Animal Care International (AAALAC; Frederick, MD, USA)-approved animal facility in our hospital with controlled temperature and light cycles (24°C and 12/12 light cycle).

2.2 Cell culture and procedure and protocol for IR injury.

H9C2 cells (BCRC 60096) were cultured in Dulbecco's modified Eagle's medium with high glucose (Gibco) containing 10% Fetal Bovine Serum (Hyclone), 100 μ g/ml streptomycin, and 100 units/ml penicillin (Gibco).

In IR experiment, H9C2 cells (i.e., 1.5×10^6 cells) were seeded in 10 cm dish. After overnight incubation, the culture medium was replaced with a serum-free one and incubated in a hypoxic incubator (i.e., 1.0% O₂ + 5.0% CO₂) for 3h. After hypoxic treatment, the culture medium was exchanged with a complete medium, followed by putting into HBO (100%) or/and treated with melatonin. After additional incubation for 24h, the cells were collected, and the protein extract was performed with RIPA buffer for western blot. For immunofluorescent (IF) stain, the same procedure was practiced but the cells were cultured in EZ Slide (Millicell). After the end of the IR/HBO procedure, the cells were fixed with 4% paraformaldehyde (PFA, Sigma) in room temperate for 15 minutes. Following the cells were blocked and permeabilized with serum and triton X-100, indicated antibodies were used for IF stain. The DAPI staining was applied for counter-staining.

2.3 Procedure and protocol of acute myocardial IR in rat.

Pathogen-free, adult male Sprague Dawley (SD) rats weighing 325-350 g (Charles River Technology, BioLASCO, Taiwan) were utilized in the present study. The procedure and protocol have been described in our previous study (30). In detail, all animals were placed in a supine position under anesthesia with 2.0% inhalational isoflurane on a warming pad at 37°C for the IR procedure. Under sterile conditions, the heart was exposed via a left thoracotomy. IR injury was induced by tightening left coronary artery for 1h at a 3 mm distal to the margin of left atrium with a 7-0 prolene suture. Regional myocardial ischemia was visually verified by observing a rapid color change from pink to dull red over the anterior surface of the left

ventricle and rapid development of akinesia and dilatation over the affected region. Rats receiving thoracotomy only without ischemia induction served as sham controls. The knot was then relieved after 1h ischemia, followed by 72h reperfusion. The rats were sacrificed at 72h after IR procedure, and hearts were harvested for individual study. The blood was collected from each animal for measuring the circulating level of endothelial progenitor cells (EPCs) prior to and at day 3 after IR induction.

2.4 Hyperbaric oxygen (HBO) therapy.

The procedure and protocol of HBO therapy were based on previous and our recent reports (31, 32). Briefly, to induce tissue-level hyperoxia, SD rats were subjected to HBO administration in an animal tabletop chamber (Piersol-Dive, model 4934) and exposed to 100% oxygen at 2.4 atmospheres for 180 minutes (3 h/one time/day for 3 consecutive days after IR procedure).

2.5 Animal grouping and strategic management.

Adult-male SD rats (n = 40) were equally categorized into five groups (n = 8 for each group): i.e., group 1 (sham-operated control, i.e., only open the chest wall, followed by closing the muscle and skin layers), group 2 (acute IR, i.e., left ventricular ischemia for 40 minutes, followed by reperfusion for 72h), group 3 (IR + HBO), group 4 [IR + Mel (50 mg/kg at 1.5h, followed administration of 20 mg/kg at days 1, 2 and 3 after IR)], and group 5 (IR + HBO + Mel). The dosage of Mel to be utilized in the present study was based on our previous reports (25, 32). Animals in each group were euthanized by day 3 after IR procedure and the heart in each animal was harvested for individual study.

2.6 Functional assessment by echocardiography.

The procedure has been reported by our previous study (30). In detail, transthoracic echocardiography was performed in each group prior to and at 72h after myocardial IR induction. The procedure was performed by an animal cardiologist blind to the experimental design using an ultrasound machine (Vevo 2100, Visualsonics). An M-mode standard two-dimensional (2D) left parasternal-long axis echocardiographic examination was conducted. Left ventricular internal dimensions [end-systolic diameter (ESD) and end-diastolic diameter (EDD)] were measured according to the American Society of Echocardiography leading-edge method using at least three consecutive cardiac cycles. Left ventricular ejection fraction (LVEF) was calculated as follows: $LVEF (\%) = [(LVEDD^3 - LVESD^3) / LVEDD^3] \times 100\%$.

2.7 Flow cytometric quantification of endothelial progenitor cells (EPCs).

Tail vein route was adopted for blood sampling at baseline and at 72 h after IR procedure. After treatment with red blood cell-lysing buffer, the remaining cells were labeled with appropriate antibodies. Flow cytometric analysis for identification of cell surface markers was performed based on our recent reports (33, 34). Briefly, the cells were immunostained for 30 minutes with monoclonal antibodies against primary antibodies, including c-kit-FITC (BD Pharmingen)/CD31-PE (BD Pharmingen), CD31-FITC (BD Pharmingen)/Sca-1-PE (R&D Systems), KDR-FITC (Abcam)/CD34-PE (BD Pharmingen), and VE-Cadherin-Alexa Flour 488 (Abcam)/CD34-PE (BD Pharmingen) (1:200). Isotype-identical antibodies (IgG) served as controls. Flow cytometric analyses were performed by utilizing a fluorescence-activated cell sorter (Beckman Coulter FC500 flow cytometer).

2.8 Immunofluorescent (IF) staining.

The procedure and protocol for IF staining have been described in our previous reports (31, 33, 34). For IF staining, rehydrated paraffin sections were first treated with 3% H₂O₂ and incubated with Immuno-Block reagent (BioSB, Santa Barbara, CA, USA) for 30 minutes at room temperature. Sections were then incubated with primary antibodies specifically against γ -H2AX (1:1000, Abcam), CD68 (1:500, Abcam), Cytochrome C (1:500, Abcam) and XRCC1/CD90 (1:200, Abcam/1:100, Abcam) at 4 °C overnight, while sections incubated with the use of irrelevant antibodies served as controls. Three sections of kidney specimen from each rat were analyzed. Alexa Fluor488, Alexa Fluor568, or Alexa Fluor594-conjugated goat anti-mouse or rabbit IgG were used to localize signals. Sections were finally counterstained with DAPI and observed with a fluorescent microscope equipped with epifluorescence (Olympus IX-40). For quantification, three random chosen HPFs (400x for IF study) were analyzed in each section. The mean number of positively stained cells per HPF for each animal was then determined by summation of all numbers divided by 9.

2.9 Western blot analysis.

The procedure and protocol for Western blot analysis have been described in previous reports (31). Briefly, equal amounts (50 μ g) of protein extracts were loaded and separated by SDS-PAGE using acrylamide gradients. After electrophoresis, the separated proteins were transferred electrophoretically to a polyvinylidene difluoride (PVDF) membrane (GE, UK). Nonspecific sites were blocked by incubation of the membrane in blocking buffer [5% nonfat dry milk in T-TBS (TBS containing 0.05% Tween 20)] overnight. The membranes were incubated with the indicated primary antibodies [vascular endothelial growth factor (VEGF) (1:1000, Abcam), CD31 (1:1000, Abcam), von Willebrand factor (vWF) (1:1000, Abcam), CXCR4 (1:1000, Abcam), stromal cell-derived growth factor (SDF)-1 α (1: 1000, Cell Signaling), hypoxia-inducible factor 1-alpha (HIF-1 α) (1:1000, Abcam) mitochondrial Bax (1: 1000, Abcam), cleaved caspase 3 (1:1000, Cell Signaling), cleaved Poly (ADP-ribose) polymerase (c-PARP) (1:1000, Cell Signaling), phosphorylated (p)-Smad3 (1: 1000, Cell Signaling), transforming growth factor (TGF)- β (1:1000, Abcam), cytosolic cytochrome C (1:2000, BD), mitochondrial cytochrome C (1:2000, BD), endothelial nitric oxide synthase (eNOS) (1: 1000, Abcam), matrix metalloproteinase (MMP)-9 (1:2000, Abcam), tumor necrosis factor (TNF)- α (1:1000, Cell Signaling), interleukin (IL)-1 β (1:1000, Cell Signaling), p-NF κ B (1:1000, Cell Signaling), NOX-1 (1:1500, Sigma-Aldrich), NOX-2 (1:1000, Sigma-Aldrich), SIRT1 (1:4000, Abcam), and SIRT3 (1:500, Abcam), and oxyblot oxidized protein detection kit (Chemicon S7150) for 1 hour at room temperature. Horseradish peroxidase-conjugated anti-rabbit immunoglobulin IgG (1:2000, Cell Signaling, Danvers, MA, USA) was used as a secondary antibody for one-hour incubation at room temperature. Actin (1:1000, Millipore) and COX IV (1:1000, Abcam) were utilized as internal controls. The washing procedure was repeated eight times within one hour. Immunoreactive bands were visualized by enhanced chemiluminescence (ECL; Amersham Biosciences, Amersham, UK) and exposed to Biomax L film (Kodak, Rochester, NY, USA). For quantification, ECL signals were digitized using Labwork software (UVP, Waltham, MA, USA).

2.10. Histological quantification of myocardial infarct and fibrotic areas.

The procedure and protocol have been described in detail in our previous reports (31, 33-35). Briefly, hematoxylin and eosin (H & E) and Masson's trichrome staining were used to identify the infarct and fibrotic areas of LV myocardium, respectively. Three serial sections of

LV myocardium in each animal were prepared at 4 μm thickness by Cryostat (Leica CM3050S). The integrated area (μm^2) of infarct area and fibrosis on each section was calculated using the Image Tool 3 (IT3) image analysis software (University of Texas, Health Science Center, San Antonio, UTHSCSA; Image Tool for Windows, Version 3.0, USA). Three randomly selected high-power fields (HPFs) (100 x) were analyzed in each section. After determining the number of pixels in each infarct and fibrotic areas per HPF, the numbers of pixels obtained from three HPFs were calculated. The procedure was repeated in two other sections for each animal. The mean pixel number per HPF for each animal was then determined by summing up all pixel numbers and divided by 9. The mean integrated area (μm^2) of fibrosis in LV myocardium per HPF was obtained using a conversion factor of 19.24 (since 1 μm^2 corresponds to 19.24 pixels). This method was also applied for identification of collagen deposition in myocardium.

2.11. Statistical analysis.

Quantitative data were expressed as mean \pm SD. Statistical analysis was adequately performed by ANOVA followed by Bonferroni multiple comparison procedure. Statistical analysis was performed using SAS statistical software for Windows version 13 (SAS Institute, Cary, NC, USA). A probability value <0.05 was considered statistically significant.

3. RESULTS

3.1. The *in vitro* study for mimicking the setting of IR injury in H9C2 cells and testing the therapeutic impact of HBO and Mel therapy.

H9C2 cells were divided into group A (H9C2 without treatment), B (H9C2 + IR), C (H9C2 + IR + HBO), D (H9C2 + IR + Mel) and E (H9C2 + IR + Mel + HBO), respectively. The result showed that the protein expressions of NOX-1 and NOX-2, indicators of oxidative stress, were significantly increased in group B compared group A. and this increase was significantly reduced in groups C, D and E compared to the group B. The level in group E was even lower than that in groups C and D., whereas the expressions of SIRT1/3, biomarkers of antioxidant, exhibited an opposite pattern to oxidative stress among the five groups (Figure 1).

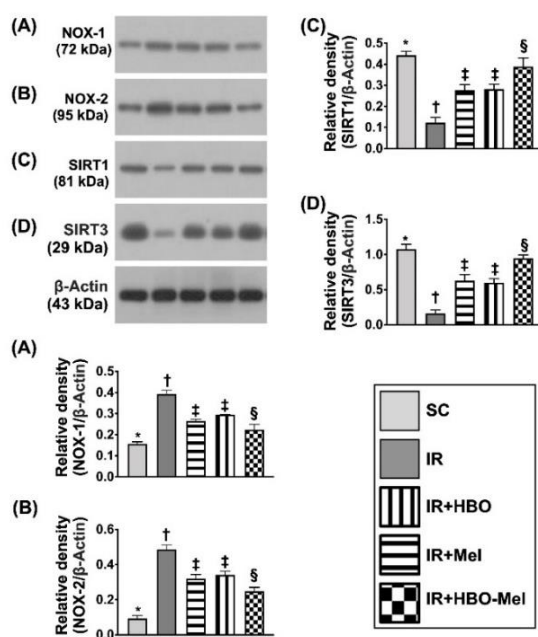


Fig. 1. The *in vitro* study for assessing the impact of HBO-Mel therapy on regulating the expressions of oxidative stress and antioxidants in H9C2 cells.

A): Protein expression of NOX-1. B): NOX-2. C): sirtuin 1 (SIRT1). D): SIRT3. ($n = 3$ for each group). Different symbols represent significant difference vs each other. SC = sham control; IR = ischemia-reperfusion; HBO = hyperbaric oxygen; Mel = melatonin.

Additionally, the protein expressions of TNF- α and NF- κ B, two indicators of inflammation, and protein expressions of mitochondrial-Bax, cleaved caspase 3 and cleaved PARP, three indicators of apoptosis, displayed an identical pattern as oxidative stress markers among the five groups (Figure 2).

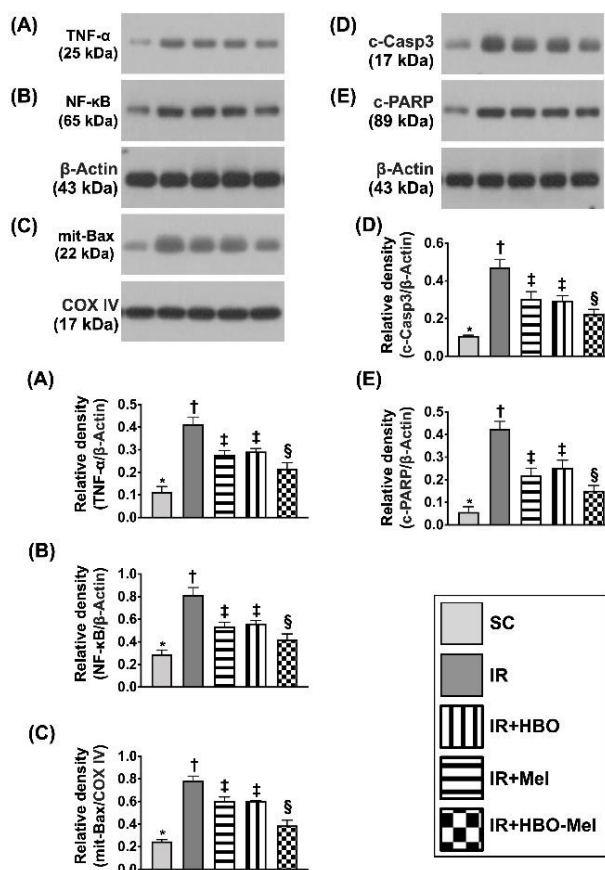


Fig. 2. The *in vitro* study for assessing the impact of HBO-Mel therapy on suppressing the expressions of inflammation and apoptosis in H9C2 cells

A): Protein expression of tumor necrosis factor (TNF)- α . B): Nuclear factor (NF)- κ B. C): Mitochondrial Bax (mit-Bax). D): Cleaved caspase 3 (c-Casp3). E): Cleaved Poly (ADP-ribose) polymerase [c-PARP ($n = 3$ for each group)]. Different symbols represent significant difference vs each other. SC = sham control; IR = ischemia-reperfusion; HBO = hyperbaric oxygen; Mel = melatonin.

Furthermore, the cellular expression of γ -H2AX (Figure 3), a double stranded DNA-damaged marker, and the cellular expression of cytosolic cytochrome C (Figure 3), a mitochondrial damaged biomarker, as well as the cellular expressions of XRCC1/CD90 (Figure 4), a single stranded DNA-damaged marker, also exhibited an identical pattern as oxidative stress markers among the five groups.

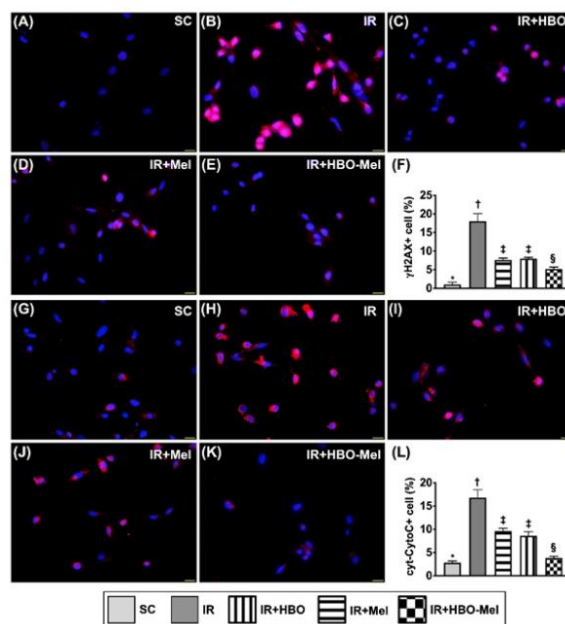


Fig. 3. The *in vitro* study for assessing the impact of HBO-Mel therapy on the cellular expressions of double stranded DNA/mitochondrial-damaged biomarkers in H9C2 cells.

A to E): Immunofluorescent (IF) images of expression of γ -H2AX (pink color) (400x). F): Analytical result of γ -H2AX+ cells, G to K): IF images of expression of cytosolic cytochrome C (cyt-CytoC) (pink color) (400x). L): Analytical result of cyt-CytoC+ cells (n = 3 for each group). Different symbols represent significant difference vs each other. SC = sham control; IR = ischemia-reperfusion; HBO = hyperbaric oxygen; Mel = melatonin.

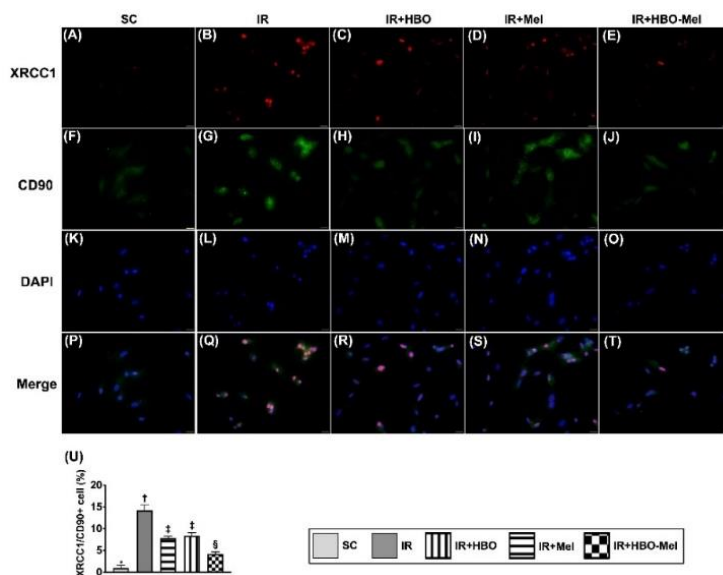


Fig. 4. The *in vitro* study for assessing the impact of HBO-Mel therapy on suppressing the cellular expressions of XRCC1/CD90.

A to E): Immunofluorescent (IF) images of XRCC1+ cells (red color) (400x). F to J): IF images of CD90+ cells (green color) (400x). K to O): IF images of DAPI+ nuclei (blue color) (400x). P to T): IF images of merged picture of double stain of the cellular expression of XRCC1/CD90 (pink color) (400x). U) Analytical results of XRCC1/CD90+ cells. (n = 3 for each group). Different symbols represent significant difference vs each other. SC = sham control; IR = ischemia-reperfusion; HBO = hyperbaric oxygen; Mel = melatonin.

3.2. Effects of HBO-Mel therapy on circulating levels of EPCs and LVEF at baseline and 72h after myocardial IR injury

To elucidate the impact of Mel and HBO therapy on circulating levels of EPCs and LVEF, we utilized the flow cytometric analysis and transthoracic echocardiographic examination. The results showed that at baseline, the circulatory numbers of EPCs (i.e., four EPCs surface markers: c-kit+/CD31+, CD31+/sca-1+, KDR+/CD34+, and VE-Cadherin+/CD34+) did not differ significantly among the five groups (Figure 5). However, at the 72h after IR injury, these parameters were highest in group 5 (IR + HBO + Mel) followed by group 4 > group 3 (IR + HBO) > group 1 (SC) > group 2 (IR) with significant difference between groups (Figure 5).

Additionally, LVEF did not differ significantly among the groups at the baseline (Figure 5). However, at the 72h after IR injury, LVEF was significantly reduced in group 2 compared to group 1. From groups 3, 4 and 5, the LVEF was significantly higher than that in group 2 with the orders group 5 > group 4 > group 3, having significant differences between groups (Figure 5).

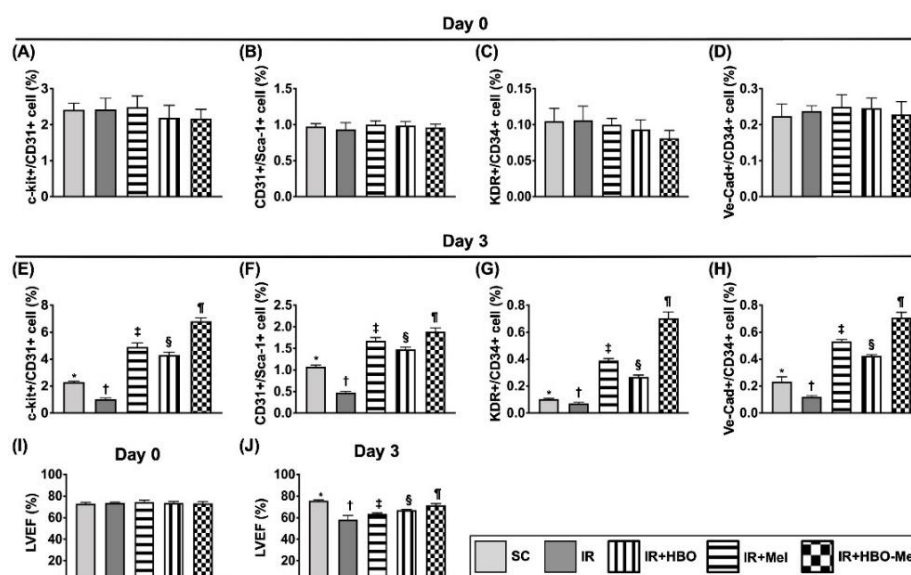


Fig. 5. Effects of HBO-Mel therapy on Circulating levels of EPCs and LVEF at the baseline of day 0 and 72h (i.e., day 3), respectively after myocardial IR injury.

A), B), C) and D): The analytical results of flow cytometric analysis of c-kit+/CD31+ cells CD31+/sca-1+ cells, KDR+/CD34+ cells and VE-Cadherin+/CD34+ cells, respectively on day 0. E), F), G) and H): The analytical results of flow cytometric analysis of c-kit+/CD31+ cells, CD31+/Sca-1+ cells KDR+/CD34+ cells and VE-Cadherin+/CD34+ cells, respectively on day 3. I) The analytical result of LVEF at day 0. J): The analytical result of LVEF on day 3, (n = 8 for each group). Different symbols represent significant difference vs each other. LVEF = left ventricular ejection fraction; EPCs = endothelial progenitor cells; SC = sham-operated control; IR = ischemia-reperfusion; HBO = hyperbaric oxygen; Mel = melatonin.

3.3. Effects of HBO-Mel therapy on protein levels of angiogenic and oxidative stress biomarkers in LV myocardium at 72h after IR injury.

The result of Western blot analysis showed that the protein expressions of SDF-1 α , CXCR4, VEGF and HIF- α , the four indices of angiogenesis, were progressively increased with significant differences from groups 1 to 5, suggesting an intrinsic response enhanced by HBO-Mel treatment to IR stimulation (Figure 6).

Additionally, the protein expressions of NOX-1, NOX-2 and oxidized protein, indicators of oxidative stress, were significantly increased in group 2 compared to the control group 1. These increases were significantly reduced in groups 3, 4 and 5 compared to the group 2. The reduced level in group 5 even significantly higher than that in groups 3 and 4 (Figure 6).

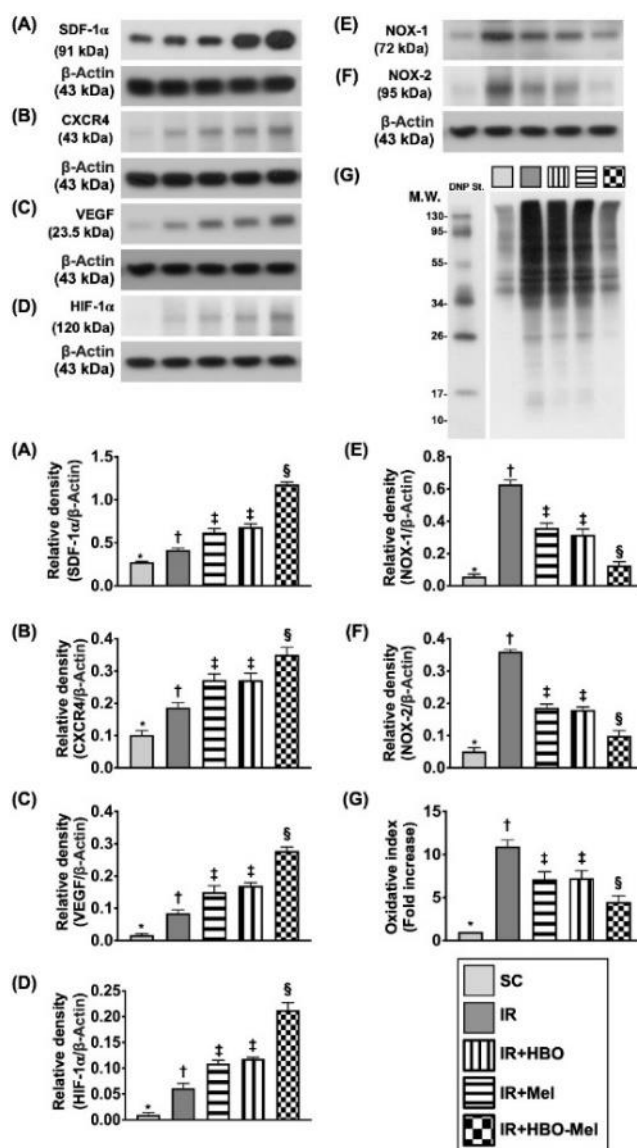


Fig. 6. Effects of HBO-Mel therapy on protein levels of angiogenic and oxidative stress biomarkers in LV myocardium at 72h after IR injury

A), B), C), D), E), and F) on the upper panel: The gel images of protein expression of stromal cell-derived factor (SDF)-1 α , CXCR4, VEGF, HIF- α , NOX-1 NOX-2, respectively. A), B), C), D), E), and F) on the low panel: their statistical data, respectively. G) on the upper panel: The gel images of oxidized protein expression detected by oxyblot protein oxidation detection kit (Note: the left and right lanes shown on the upper panel represent protein molecular weight marker and control oxidized molecular protein standard, respectively). G) on the low panel: Their statistical data. ($n = 6$ for each group). Different symbols represent significant difference vs each other. M.W. = molecular weight; DNP = 1-3 dinitrophenylhydrazone. IR = ischemia-reperfusion; HBO = hyperbaric oxygen; Mel = melatonin.

3.4. Effects of HBO-Mel therapy on protein expressions of apoptotic, fibrotic and inflammatory biomarkers in LV myocardium at 72h after IR injury.

The protein expressions of mitochondrial-Bax, cleaved-caspase-3 and cleaved-PARP, three indicators of apoptosis, were significantly increased in group 2 compared to the control group 1. These increases were significantly reduced in groups 3, 4 and 5 compared to the group 2 with significantly lower in group 5 than in that of groups 3 and 4. The cleaved caspase 3 was lower in group 4 than in that group 3 (Figure 7). Additionally, the protein expressions of TGF- β and Smad3, two indicators of fibrosis, displayed a similar pattern as apoptosis among the five groups (Figure 7). Furthermore, the protein expressions of IL-1 β , TNF- α and MMP-9, three indicators of inflammation, also displayed a similar pattern as apoptosis among the five groups (Figure 7).

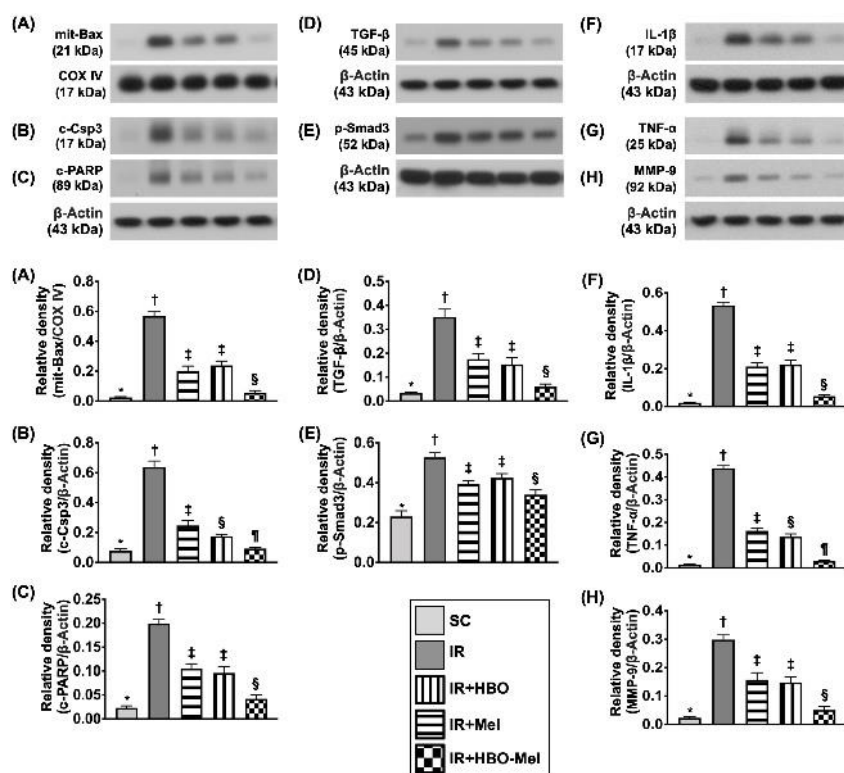


Fig. 7. Effects of HBO-Mel therapy on protein expressions of apoptotic, fibrotic and inflammatory biomarkers in LV myocardium at 72h after IR injury.

A), B), C), D), E), F), G), H) on the upper panel: The gel images of protein expression of mit-Bax, c-Casp3, c-PARP, TGF- β , (p)-Smad3, IL-1 β , TNF- α , matrix metalloproteinase (MMP)-9, respectively. A), B), C), D), E), F), G), H) on the low panel, their statistically analyzed data, respectively. ($n = 6$ for each group). Different symbols represent significant difference vs each other. IR = ischemia-reperfusion; HBO = hyperbaric oxygen; Mel = melatonin.

3.5. Effects of HBO-Mel therapy on protein expressions of endothelial cell and mitochondrial-damaged biomarkers in LV myocardium by 72h after IR injury.

The protein expressions of CD31, vWF and eNOS, three indices of endothelial cell functional integrity, were significantly decreased in group 2 compared to the control group 1. These decreases were significantly diminished in groups 3, 4 and 5 compared to the group 2 and the significantly less decrease in group 5 than that in groups 3 and 4 was observed.

(Figure 8). The protein expression of mitochondrial cytochrome C, an indicator of mitochondrial integrity, displayed an identical pattern as CD31 among the groups (Figure 8), whereas the protein expression of cytosolic cytochrome C, an indicator of mitochondrial damaged biomarker, exhibited an opposite pattern as CD31.

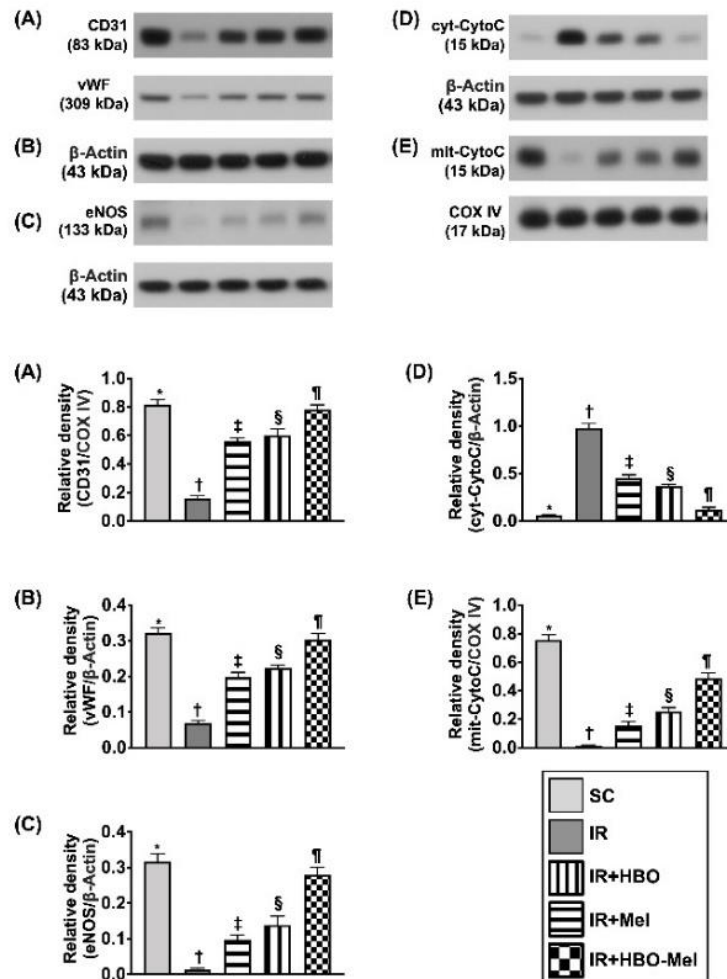


Fig. 8. Effects of HBO-Mel therapy on protein expressions of endothelial cell and mitochondrial-damaged biomarkers in LV myocardium at 72h after IR injury.

A), B), C), D) and E) on the upper panel: The gel images of protein expression of CD31, * vWF, eNOS, cyt-CytoC and mit-CytoC, respectively. A), B), C), D) and E) on the low panel: Their statistical data, respectively ($n = 6$ for each group). Different symbols represent significant difference vs each other. SC = sham-operated control; IR = ischemia-reperfusion; HBO = hyperbaric oxygen; Mel = melatonin.

3.6. Effects of HBO-Mel therapy on infarct and fibrotic areas in LV myocardium at 72h after IR injury.

The result demonstrated that the infarct area was significantly increased in group 2 compared to the control group 1. The increased infarct area induced by IR was significantly lower in groups 3, 4 and 5 than that of group 2, in which group 5 was even significantly lower than that in groups 3 and 4 (Figure 9). Additionally, the fibrotic area exhibited an identical pattern as the infarct area mentioned above among the five groups (Figure 9).

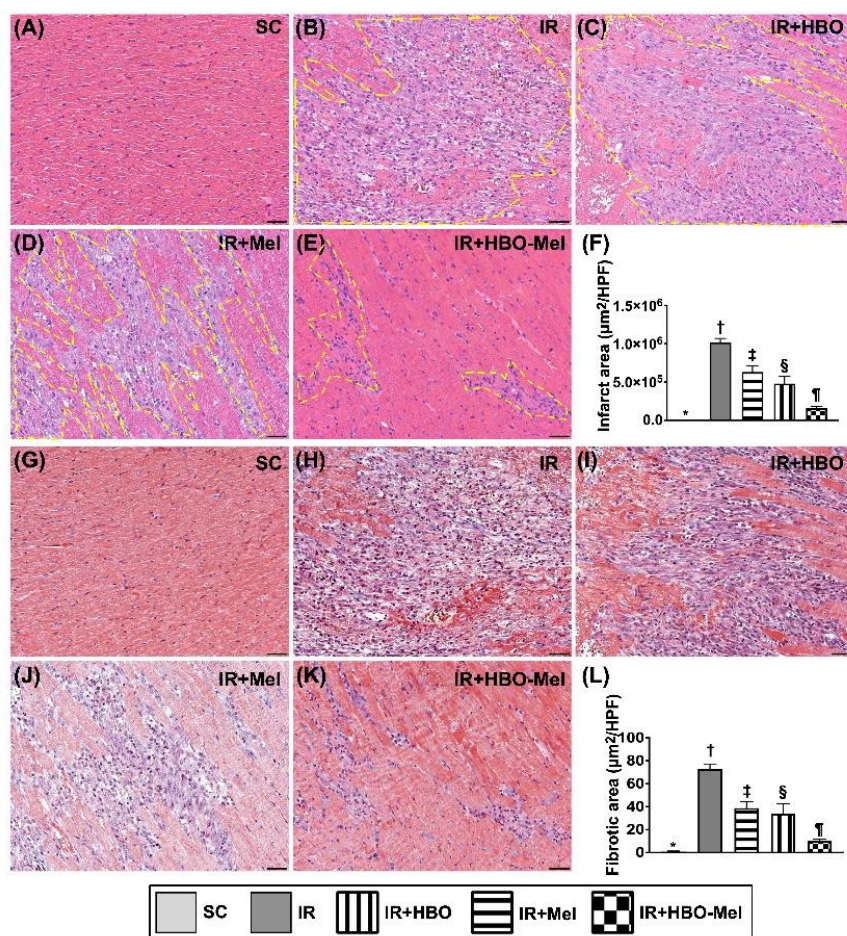


Fig. 9. Effects of HBO-Mel therapy on infarct and fibrotic areas in LV myocardium at 72h after IR injury.

A to E): The representative images of the microscopic finding (200x) of cardiac infarct area (darkish color) (yellowish dotted lines) for SC, IR, R+HBO, R+Mel, R+HBO+Mel, respectively. *F):* Analytical result of infarct area of these groups, respectively. *G to K):* The representative images of microscopic finding (200x) of cardiac fibrotic area (blue color) for SC, IR, R+HBO, R+Mel, R+HBO+Mel, respectively. *L):* Analytical result of fibrotic area of these groups, respectively. Scale bar in right lower corner represents 50 μm . ($n = 6$ for each group). Different symbols represent significant difference vs each other. LV = left ventricular; SC = sham-operated control; IR = ischemia-reperfusion; HBO = hyperbaric oxygen; Mel = melatonin.

3.7. Effects of HBO-Mel therapy on cellular levels of DNA-damaged and inflammatory biomarkers in LV myocardium by 72h after IR injury.

The expression of $\gamma\text{-H2AX}$, an indicator of DNA-damaged marker, and CD68, an indicator of inflammation, were significantly elevated in group 2 compared to the control group 1. These elevations induced by RI were significantly reduced in groups 3, 4 and 5 compared to the group 2. This reduction in group 5 was even significantly greater than that in groups 3 (Figure 10).

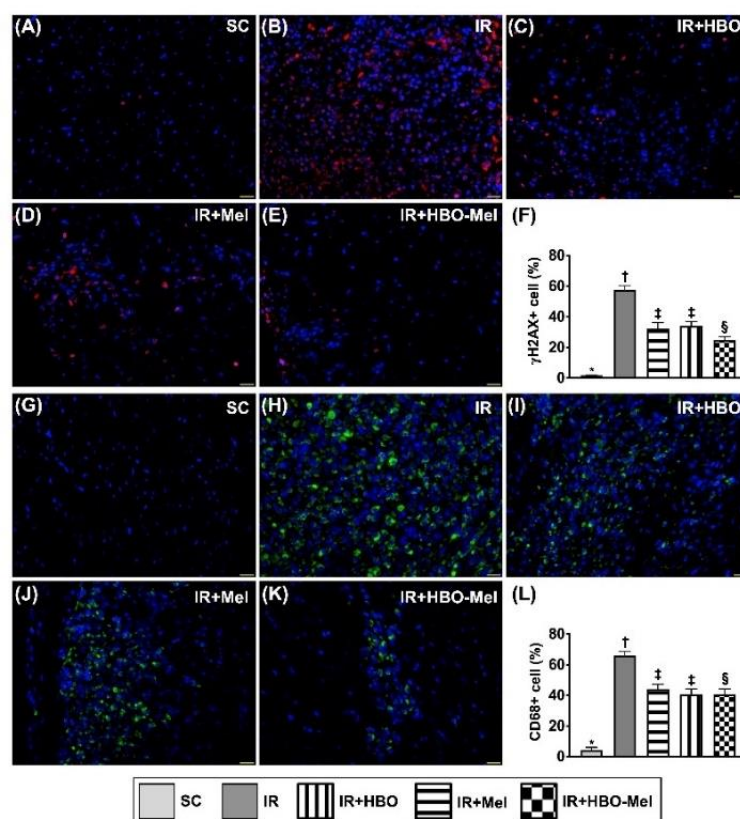


Fig. 10. Cellular expressions of DNA-damaged and inflammatory biomarkers in LV myocardium by 72h after IR injury.

A to E): The representative images of the immunofluorescent (IF) microscopic finding of γ -H2AX+ cells (pink color) for SC, IR, R+HBO, R+Mel, R+HBO+Mel, respectively (400x). *F):* Analytical result of γ -H2AX+ cells for these groups, respectively. *G to K):* The representative images of IF microscopic finding of cellular expression of CD68 (green color) for SC, IR, R+HBO, R+Mel, R+HBO+Mel, respectively. *L):* Analytical result of CD68+ cells for these groups, respectively. ($n = 6$ for each group). Different symbols represent significant difference vs each other. SC = sham-operated control; IR = ischemia-reperfusion; HBO = hyperbaric oxygen; Mel = melatonin.

4. DISCUSSION

In this study the therapeutic impact of Mel-HBO on myocardial IR injury was investigated and the results yielded several preclinical striking implications. First, mechanisms of the myocardial damage induced by IR were extremely complicated, i.e., involving in inflammatory reaction, oxidative stress, apoptosis, DNA and mitochondrial damages as well as fibrosis. Second, HBO and Mel offered a comparable effect on protecting myocardium against IR injury, respectively. Third, the combined HBO and Mel therapy was identified to offer a synergic effect on protecting the myocardium against IR injury, resulting in preserving the LVEF in rats.

Our previous studies (19, 20, 22-25) have shown that Mel therapy effectively protected the organs from IR injury. Additionally, our recent studies (27, 32, 36) have demonstrated that HBO therapy remarkably protected the organs from IR injury. In the present study we confirmed that either HBO or melatonin treatment remarkably preserved LVEF in IR animals. The most important finding in the present study was that the combined HBO-Mel therapy was superior to HBO or melatonin either one alone on preserving the LVEF in IR rat, suggesting

the synergic effect of this combined regimen. Our finding, in addition to corroborating with the finding of previous (19, 20, 22-25) and recent (27, 32, 36) studies, highlighting that this combined regimen may have therapeutic potential for patients with acute myocardial IR injury, especially who are refractory to conventional treatment.

It is well known that organ IR injury always elicits vigorous inflammatory reaction and generations of free radicals which in turn further damage the organs (19, 20, 22-25, 27, 32, 36). Our *in vitro* and *in vivo* studies further confirmed the markedly upregulated inflammatory reaction and oxidative stress in the setting of IR injury. In this way, our findings were consistent with the findings from the previous studies (19, 20, 22-25). These findings could, at least in part, explain why the apoptosis, DNA/mitochondrial damages and fibrosis were significantly increased and heart function was notably reduced in IR animals as compared with those of the SC animals. It is well documented that Mel treatment significantly reduces inflammation and oxidative stress in IR organs and sepsis syndrome (19, 22, 23). The similar results have been observed in the current IR animal model with Mel treatment; however, the protective effect is even greater when the combined HBO-Mel treatment is used. The findings not only corroborate with the previous studies (19, 22, 23), but also at least in part, explain why the HBO-Mel treatment can effectively preserve the LVEF in IR animal model.

The association between organ ischemia/IR injury with DNA and mitochondrial damages and cellular apoptosis has been extensively investigated (31-33, 36, 37). In the present study, we also found that the above mentioned molecular-cellular perturbations were substantially increased in IR animals. These molecular-cellular perturbations caused by the IR inevitably reduces LVEF. Either HBO or Mel treatment alone provided partial protective effects on these perturbations. Therefore, their combination provided better protection than that of their each alone to the IR injuries, including LVEF.

Angiogenesis and neovascularization play essential roles for recovery of ischemia-related organ dysfunction (36, 38-40). An essential finding in the present study was that the circulating level of EPCs was notably reduced in IR animals than in SC counterparts. Our finding was consistent with the finding of the previous studies (36, 38-40). However, this defect was notably reversed by HBO or Mel treatment alone, but more effectively prevented by combined HBO-Mel treatment. In addition, the expressions of the angiogenesis biomarkers in the LV myocardium were remarkably reduced in IR animals and this reduction was significantly diminished by the combined HBO-Mel treatment. These findings provided additional evidence to support to use of HBO-Mel combination to treat IR injury

The therapeutic impact of HBO on protecting the organ against ischemia/IR injury has been keenly investigated (41, 42). However, the main concern remains that the HBO therapy may enhance the generation of ROS with oxidative damages to the cells, tissues and organs. While, Mel, as a potent and durable free radical scavenger (21) has the capacity to counterbalance the side effect of the HBO therapy. In addition, their protective effects may exhibit a synergic effect and this synergic effect has been observed in the current study, i.e., the superior protective effects of HBO-Mel on LV myocardium IR injury over the melatonin or HBO alone. Mechanistically, the HBO-Mel therapy enhances the mobilization of the EPCs from bone marrow into circulation and homes them into the ischemic zone for angiogenesis. HBO-Mel therapy also downregulates the inflammatory reaction and the oxidative stress, resulting in attenuating the mitochondrial/DNA damages, and ultimately inhibited the LV fibrosis and LV remodeling. The potential mechanism has been illustrated in the Figure 11.

Although the results were attractive and promising, the shortcomings of the study are present. First, the study period was only 72h and it would not provide important information as to whether HBO-Mel therapy could ensure the long-lasting protective effect on the heart IR injury. Second, although extensive works were done by the present study, the exact underlying mechanism related to myocardium damage and reduced the LVEF caused by IR was still not

yet keenly investigated. These are the goals of our future studies.

In conclusion, the results of the present study revealed that the combined HBO and Mel therapy was superior to either one alone for preserving the LVEF in acute heart IR injury.

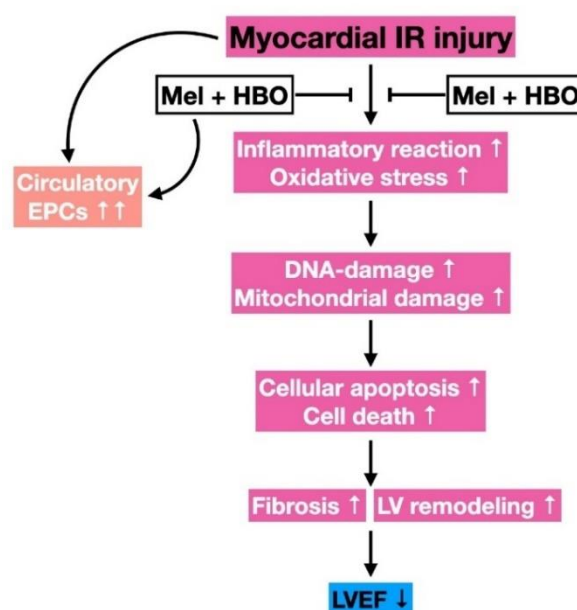


Fig. 11. The proposed underlying mechanisms regarding how the HBO-Mel therapy on protection of the heart from IR injury.

IR = ischemia-reperfusion; HBO = hyperbaric oxygen; Mel = melatonin; LVEF = left ventricular ejection fraction.

ABBREVIATION

c-PARP	cleaved poly (ADP-ribose) polymerase
cyt-CytoC	cytosolic cytochrome C
EPCs	endothelial progenitor cells
eNOS	endothelial nitric oxide synthase
HIF- α	hypoxia inducible factor alpha
IL-1 β	interleukin 1 beta
IR	ischemia reperfusion
IF	immunofluorescent
LVEF	left ventricular ejection fraction
mit-Bax	mitochondrial Bax
mit-CytoC	mitochondrial cytochrome C
MMP-9	matrix metalloproteinase 9
Mel	melatonin
TNF- α	tumor necrosis factor alpha
NF- κ B	nuclear factor-kappa B
SIRT	sirtuin
SDF-1 α	stromal cell-derived factor 1 alpha
TGF- β	transforming growth factor beta
vWF	von Willebrand factor
VEGF	vascular endothelial growth factor

ACKNOWLEDGMENTS

We thank the molecular imaging core of the Institute for Translational Research in Biomedicine, Kaohsiung Chang Gung Memorial Hospital, Kaohsiung, Taiwan, for technical and facility supports on Echo Vevo 2100. This study was supported by a program grant from Chang Gung Memorial Hospital, Chang Gung University [CMRPG8H0821].

AUTHORSHIP

Conceptualization, HKY and HTC; Methodology, HTC, JNY and PHS; Validation, JNY and HKY; Formal Analysis, HTC, JNY and PHS; Investigation, HTC, JNY, FYL and PHS; Data Curation, HTC, JNY, FYL and PHS; Writing – Original Draft Preparation, HTC and HKY; Writing – Review & Editing, JYC and HKY; Supervision, FYL and HKY; Project Administration, FYL; Funding Acquisition, FYL. All authors read and approved the final manuscript.

CONFLICTS OF INTEREST:

The authors declare no conflict of interest.

REFERENCES

1. Cheruvu C *et al.* (2016) Long term prognostic utility of coronary CT angiography in patients with no modifiable coronary artery disease risk factors: Results from the 5 year follow-up of the CONFIRM International Multicenter Registry. *J. Cardiovasc. Comput. Tomogr.* **10** (1): 22-27.
2. Roth GA *et al.* (2017) Global, regional, and national burden of cardiovascular diseases for 10 causes, 1990 to 2015. *J. Am. Coll. Cardiol.* **70** (1): 1-25.
3. Fischer Q *et al.* (2018) Optimal long-term antithrombotic treatment of patients with stable coronary artery disease and atrial fibrillation: "OLTAT registry". *Int. J. Cardiol.* **264**: 64-69.
4. Gharacholou SM *et al.* (2018) Characteristics and long term outcomes of patients with acute coronary syndromes due to culprit left main coronary artery disease treated with percutaneous coronary intervention. *Am. Heart J.* **199**: 156-162.
5. Medina-Inojosa JR *et al.* (2018) Association between adiposity and lean mass with long-term cardiovascular events in patients with coronary artery disease: No paradox. *J. Am. Heart Assoc.* **7** (10): e007505.
6. Kloner RA, Ellis SG, Lange R, Braunwald E (1983) Studies of experimental coronary artery reperfusion. Effects on infarct size, myocardial function, biochemistry, ultrastructure and microvascular damage. *Circulation* **68** (2 Pt 2): I8-15.
7. Ito H *et al.* (1996) Clinical implications of the 'no reflow' phenomenon. A predictor of complications and left ventricular remodeling in reperfused anterior wall myocardial infarction. *Circulation* **93** (2): 223-228.
8. Chen Y S *et al.* (2003) Analysis and results of prolonged resuscitation in cardiac arrest patients rescued by extracorporeal membrane oxygenation. *J. Am. Coll. Cardiol.* **41** (2): 197-203.
9. Rokos IC *et al.* (2006) Rationale for establishing regional ST-elevation myocardial infarction receiving center (SRC) networks. *Am. Heart J.* **152** (4): 661-667.
10. Rokos IC *et al.* (2009) Integration of pre-hospital electrocardiograms and ST-elevation myocardial infarction receiving center (SRC) networks: impact on Door-to-Balloon times across 10 independent regions. *JACC Cardiovasc. Interv.* **2** (4): 339-346.

11. Braunwald E, Kloner RA (1985) Myocardial reperfusion: a double-edged sword? *J. Clin. Invest.* **76** (5): 1713-1719.
12. De Scheerder I *et al.* (1985) Post-cardiac injury syndrome and an increased humoral immune response against the major contractile proteins (actin and myosin). *Am. J. Cardiol.* **56** (10): 631-633.
13. Frangogiannis NG (2008) The immune system and cardiac repair. *Pharmacol. Res.* **58** (2): 88-111.
14. Frangogiannis NG, Smith CW, Entman ML (2002) The inflammatory response in myocardial infarction. *Cardiovasc. Res.* **53** (1): 31-47.
15. Lambert JM, Lopez EF, Lindsey ML (2008) Macrophage roles following myocardial infarction. *Int. J. Cardiol.* **130** (2): 147-158.
16. Lange LG, Schreiner GF (1994) Immune mechanisms of cardiac disease. *N. Engl. J. Med.* **330** (16): 1129-1135.
17. Moens AL, Claeys MJ, Timmermans JP, Vrints CJ (2005) Myocardial ischemia/reperfusion-injury, a clinical view on a complex pathophysiological process. *Int. J. Cardiol.* **100** (2): 179-190.
18. Yellon DM, Hausenloy DJ (2007) Myocardial reperfusion injury. *N. Engl. J. Med.* **357** (11): 1121-1135.
19. Chang CL *et al.* (2015) Protective effect of melatonin-supported adipose-derived mesenchymal stem cells against small bowel ischemia-reperfusion injury in rat. *J. Pineal Res.* **59** (2): 206-220.
20. Chen HH *et al.* (2014) Additional benefit of combined therapy with melatonin and apoptotic adipose-derived mesenchymal stem cell against sepsis-induced kidney injury. *J. Pineal Res.* **57** (1): 16-32.
21. Manchester LC *et al.* (2015) Melatonin: an ancient molecule that makes oxygen metabolically tolerable. *J. Pineal Res.* **59** (4): 403-419.
22. Sun CK *et al.* (2015) Systemic combined melatonin-mitochondria treatment improves acute respiratory distress syndrome in the rat. *J. Pineal Res.* **58** (2): 137-150.
23. Yip HK *et al.* (2015) Combined melatonin and exendin-4 therapy preserves renal ultrastructural integrity after ischemia-reperfusion injury in the male rat. *J. Pineal Res.* **59** (4): 434-447.
24. Chen HH *et al.* (2016) Melatonin pretreatment enhances the therapeutic effects of exogenous mitochondria against hepatic ischemia-reperfusion injury in rats through suppression of mitochondrial permeability transition. *J. Pineal Res.* **61** (1): 52-68.
25. Sun CK *et al.* (2017) Melatonin treatment enhances therapeutic effects of exosomes against acute liver ischemia-reperfusion injury. *Am. J. Transl. Res.* **9** (4): 1543-1560.
26. Slovut DP, Sullivan TM (2008) Critical limb ischemia: medical and surgical management. *Vasc. Med.* **13** (3): 281-291.
27. Ko SF *et al.* (2020) Protective effect of combined therapy with hyperbaric oxygen and autologous adipose-derived mesenchymal stem cells on renal function in rodent after acute ischemia-reperfusion injury. *Am. J. Transl. Res.* **12** (7): 3272-3287.
28. Lin PY *et al.* (2018) Hyperbaric oxygen therapy enhanced circulating levels of endothelial progenitor cells and angiogenesis biomarkers, blood flow, in ischemic areas in patients with peripheral arterial occlusive disease. *J. Clin. Med.* **7** (12) :548.
29. Thom SR (2011) Hyperbaric oxygen: its mechanisms and efficacy. *Plast. Reconstr. Surg.* **127** Suppl 1: 131S-141S.
30. Lee FY *et al.* (2018) Combined therapy with SS31 and mitochondria mitigates myocardial ischemia-reperfusion injury in rats. *Int. J. Mol. Sci.* **19** (9): 2782.
31. Hsu SL *et al.* (2019) Hyperbaric oxygen facilitates the effect of endothelial progenitor cell therapy on improving outcome of rat critical limb ischemia. *Am. J. Transl. Res.* **11** (4):

1948-1964.

32. Lin KC *et al.* (2019) Combined therapy with hyperbaric oxygen and melatonin effectively reduce brain infarct volume and preserve neurological function after acute ischemic infarct in rat. *J. Neuropathol. Exp. Neurol.* **78** (10): 949-960.
33. Chua S *et al.* (2014) Inhibition of dipeptidyl peptidase-IV enzyme activity protects against myocardial ischemia-reperfusion injury in rats. *J. Transl. Med.* **12**: 357.
34. Yeh KH *et al.* (2012) Benefit of combined extracorporeal shock wave and bone marrow-derived endothelial progenitor cells in protection against critical limb ischemia in rats. *Crit. Care Med.* **40** (1): 169-177.
35. Lu HI *et al.* (2017) SS31 therapy effectively protects the heart against transverse aortic constriction-induced hypertrophic cardiomyopathy damage. *Am. J. Transl. Res.* **9** (12): 5220-5237.
36. Chen YC *et al.* (2020) Circulatory rejuvenated EPCs derived from PAOD patients treated by CD34(+) cells and hyperbaric oxygen therapy salvaged the nude mouse limb against critical ischemia. *Int. J. Mol. Sci.* **21** (21): 7887.
37. Ko SF, Huang TH, Lin YP, Chen YL, Yip HK (2022) Accuracy and precision of 31P-MRS assessment for evaluating the effect of melatonin-pretreated mitochondria transferring on liver fibrosis of rats. *Melatonin Res.* **5** (1): 18-33.
38. Lee FY *et al.* (2015) Intracoronary Transfusion of circulation-derived CD34+ cells improves left ventricular function in patients with end-stage diffuse coronary artery disease unsuitable for coronary intervention. *Crit. Care Med.* **43** (10): 2117-2132.
39. Sung PH *et al.* (2018) The five-year clinical and angiographic follow-up outcomes of intracoronary transfusion of circulation-derived CD34+ cells for patients with end-stage diffuse coronary artery disease unsuitable for coronary intervention-phase i clinical trial. *Crit. Care Med.* **46** (5): e411-e418.
40. Yin TC *et al.* (2019) Extracorporeal shock wave-assisted adipose-derived fresh stromal vascular fraction restores the blood flow of critical limb ischemia in rat. *Vascul. Pharmacol.* **113**: 57-69.
41. Ni XX *et al.* (2020) Protective effects of hyperbaric oxygen therapy on brain injury by regulating the phosphorylation of Drp1 through ROS/PKC pathway in heatstroke rats. *Cell Mol. Neurobiol.* **40** (8): 1253-1269.
42. Zhang Y *et al.* (2013) Hyperbaric oxygen therapy in rats attenuates ischemia-reperfusion testicular injury through blockade of oxidative stress, suppression of inflammation, and reduction of nitric oxide formation. *Urology* **82** (2): 489 e489-489 e415.



This work is licensed under a [Creative Commons Attribution 4.0 International License](https://creativecommons.org/licenses/by/4.0/)

Please cite this paper as:

Chai, H.-T., Yeh, J.-N., Sung, P.-H., Chiang, J.Y., Lee, F.-Y. and Yip, H.-K. 2022. Hyperbaric oxygen-assisted melatonin therapy protects the heart from acute ischemia-reperfusion injury. *Melatonin Research.* **5**, **2** (Jun. 2022), **114-132**. DOI:<https://doi.org/https://doi.org/10.32794/mr112500124>.